Cobalt(2+) Binding to Human and Tomato Copper Chaperone for Superoxide Dismutase: Implications for the Metal Ion Transfer Mechanism † , ‡

ARTICLE *in* BIOCHEMISTRY · JUNE 2000

Impact Factor: 3.02 · DOI: 10.1021/bi992727+ · Source: PubMed

9 AUTHORS, INCLUDING:

Amir Liba
Agilent Technologies
9 PUBLICATIONS **308** CITATIONS
SEE PROFILE

P. John Hart
University of Texas Health Science Center at …
109 PUBLICATIONS **4,118** CITATIONS
SEE PROFILE

Edith B Gralla
University of California, Los Angeles
92 PUBLICATIONS **7,497** CITATIONS
SEE PROFILE

Cobalt(2+) Binding to Human and Tomato Copper Chaperone for Superoxide Dismutase: Implications for the Metal Ion Transfer Mechanism[†,‡]

Haining Zhu,[§] Eric Shipp,[§] Raylene J. Sanchez,[§] Amir Liba,[§] Jennifer E. Stine,[||] P. John Hart,[||] Edith B. Gralla,[§] Aram M. Nersissian,[§] and Joan Selverstone Valentine*[,§]

Department of Chemistry and Biochemistry, University of California, Los Angeles, California 90095-1569, and Center for Biomolecular Structure Analysis, Department of Biochemistry, University of Texas Health Science Center at San Antonio, 7703 Floyd Curl Drive, San Antonio, Texas 78284-7760

Received November 29, 1999; Revised Manuscript Received February 8, 2000

ABSTRACT: The copper chaperone for superoxide dismutase (*CCS*) gene encodes a protein that is believed to deliver copper ions specifically to copper−zinc superoxide dismutase (CuZnSOD). CCS proteins from different organisms share high sequence homology and consist of three distinct domains; a CuZnSOD-like central domain 2 flanked by domains 1 and 3, which contain putative metal-binding motifs. We report deduced protein sequences from tomato and *Arabidopsis*, the first functional homologues of CCS identified in plants. We have purified recombinant human (hCCS) and tomato (tCCS) copper chaperone proteins, as well as a truncated version of tCCS containing only domains 2 and 3. Their cobalt(2+) binding properties in the presence and absence of mercury(2+) were characterized by UV−vis and circular dichroism spectroscopies and it was shown that hCCS has the ability to bind two spectroscopically distinct cobalt ions whereas tCCS binds only one. The cobalt binding site that is common to both hCCS and tCCS displayed spectroscopic characteristics of cobalt(2+) bound to four or three cysteine ligands. There are only four cysteine residues in tCCS, two in domain 1 and two in domain 3; all four are conserved in other CCS sequences including hCCS. Thus, an interaction between domain 1 and domain 3 is concluded, and it may be important in the copper chaperone mechanism of these proteins.

CCS[1] is a member of a novel class of proteins, termed copper chaperones, that are involved in intracellular trafficking and delivery of copper to copper-containing proteins. The mechanisms by which these copper chaperones function are not known in detail but are presumed to involve highly specific molecular recognition between delivery (donor) and target (acceptor) proteins (*1*−*3*). *CCS* was originally identified as a gene involved in lysine biosynthesis in *Saccharomyces cerevisiae* and was designated *LYS7* (*4*). Subsequently, *LYS7* was cloned and characterized by Sprague and coworkers (*5*), and evidence was presented suggesting that it functions outside of lysine biosynthesis. The gene for a similar protein was recently identified in humans, and it was postulated that it escorts and transfers copper specifically to CuZnSOD. Hence it was designated as copper chaperone for superoxide dismutase (*CCS*) (*1*). This suggestion was originally based on the fact that the *lys7* null strain of *S. cerevisiae* displays numerous phenotypes that are identical to those seen in the *sod1* null strains (*1*, *6*). In support of this conclusion, it was recently shown that the CuZnSOD protein isolated from the *lys7* null strain of *S. cerevisiae* is entirely devoid of copper (*7*).

Both human CCS and yeast Lys7 are multidomain proteins displaying strikingly similar domain organization. The N-terminal domain (domain 1, approximately 80 amino acids) has high sequence homology to the ATX1 proteins (*8*−*11*); to MerP, a gene product involved in mercury resistance in some prokaryotes (*12*); and to similar domains found within the CPx-type heavy metal transporting ATPases (*13*−*15*). Recent structural studies have revealed that the ATX1 protein and homologous domains have a similar folding topology, known as a ferredoxin-like fold, and carry a flexible metal-binding loop containing a consensus MXCXXC sequence motif (*16*−*19*).

The N-terminal domain is followed by a 153 amino acid domain (domain 2), which displays sequence homology to its target protein CuZnSOD. It is worth noting that hCCS, based on amino acid sequence alignment, apparently main-

[†] This work was supported by a grant from the National Institute of General Medical Sciences GM28222 (J.S.V.) and in part by grants from the Robert A. Welch Foundation, the UTHSCSA Research Resources Program for Medical Schools of the Howard Hughes Medical Institute, and the UTHSCSA Competitive Research Enhancement Fund for New Faculty (P.J.H.).

[‡] The nucleotide sequences for tomato and *Arabidopsis* CCS reported in this paper have been deposited in GenBank under accession numbers AF117707 and AF179371, respectively.

* To whom correspondence should be addressed: Fax (310) 206-7197; Email jsv@chem.ucla.edu.

[§] UCLA.

[||] University of Texas Health Science Center at San Antonio.

[1] Abbreviations: CCS, copper chaperone for copper−zinc superoxide dismutase; h-, t-, and ArCCS, human, tomato, and *Arabidopsis* copper chaperones for copper−zinc superoxide dismutase; Lys7, yeast copper chaperone for copper−zinc superoxide dismutase; tCCS-D2D3, truncated protein containing domains 2 and 3 of tomato copper chaperone for copper−zinc superoxide dismutase; CuZnSOD, copper−zinc superoxide dismutase; (F)ALS, (familial) amyotrophic lateral sclerosis; EST, expressed sequence tag; CD, circular dichroism; UV−vis, ultraviolet−visible; IPTG, isopropyl thiogalactoside; SDS−PAGE, sodium dodecyl sulfate−polyacrylamide gel electrophoresis; DEAE, diethylaminoethyl; DTT, dithiothreitol; S_2-*o*-xyl, bis(*o*-xylyl-α,α′-dithiolato).

10.1021/bi992727+ CCC: $19.00
Published on Web 04/09/2000

tains an intact zinc site and a slightly modified copper site (an Asp residue replaces the His120 ligand of CuZnSOD) in its domain 2. A recent crystal structural study of domain 2 of hCCS revealed the presence of Zn^{2+} at that zinc site (*20*). Interestingly, yeast Lys7 is fully functional as a copper chaperone for CuZnSOD despite the fact that it does not possess any metal binding site in domain 2. The C-terminal domain (domain 3) is relatively short, 30−40 residues, and carries two conserved cysteine residues that are one residue apart and may play a crucial role in metal transfer to CuZnSOD. The yeast Lys7 domain 2 alone (*21*) and full-length (*22*) structures have recently been solved and revealed that domains 1 and 2 do resemble the fold of ATX1 and CuZnSOD respectively; unfortunately, domain 3 remained disordered in the crystal structure (*22*).

It has been postulated recently, on the basis of in vivo complementation studies, that domain 2 harbors the site(s) responsible for the protein−protein interaction between CuZnSOD and CCS, while domains 1 and 3 are cooperatively involved in copper binding and incorporation into CuZnSOD (*23*). However, the same series of experiments also showed that complementation still could be achieved with a construct lacking domain 1, while domain 3 appeared to be indispensable for the functional activity of CCS (*23*). Four cysteine residues are found to be conserved in all known CCS proteins, two in the consensus heavy metal binding motif MXCXXC in domain 1 and two other in the CXC motif in domain 3. These four conserved cysteine residues are potential candidates for metal ion binding site(s) and are likely to play important roles in the copper chaperone function.

The detailed molecular mechanism by which CCS enables metalation of CuZnSOD by copper, as well as whether it plays a role in the mutant CuZnSOD-induced ALS pathology, remain unknown. We have expressed and purified hCCS in order to study the mechanism of CCS-induced metalation of wild-type human CuZnSOD and to test for possible abnormal interactions with FALS mutant human CuZnSODs (*24, 25*). In addition, we have expressed and purified tCCS, both for comparative studies with hCCS and because of our interest in copper proteins in plants (*26*−*28*). We report here the results of the initial phase of this investigation in which we have characterized the metal binding properties of hCCS and tCCS using Co^{2+} as a probe because of its proven utility as a reporter of the nature of metal ion binding sites in zinc and copper proteins (*29, 30*).

EXPERIMENTAL PROCEDURES

Cloning and Construction of Expression Vectors. ESTs encoding *Arabidopsis* and tomato CCS were identified in the GenBank/dbest database by using the LYS7 sequence for a TBLASTN homology search. Corresponding cDNA clones were obtained from the *Arabidopsis* Biological Resource Center at The Ohio State University and from the Department of Plant Breeding, Cornell University, Ithaca, NY. The complete nucleotide sequences were determined for both strands at the UCLA DNA sequencing facility and deposited in the GenBank database (accession numbers AF117707 for tCCS and AF179371 for ArCCS). The plasmid harboring cDNA encoding full-length hCCS (pSMCCS) was kindly provided to us by Dr. V. C. Culotta, Johns Hopkins University School of Public Health, Baltimore, MD.

The EST clones encoding tCCS and ArCCS appear to encode incomplete precursors for chloroplast proteins on the basis of the following reasoning: (1) The open reading frames in both tCCS and ArCCS clones can be extended without interruption for additional 71 (tCCS) and 56 (ArCCS) codons upstream of the potential translational initiation sites, which is Met 72 in tomato and Met 57 in *Arabidopsis*. (2) The nucleotide sequences flanking the putative AUG initiator codons do not display the characteristics of a strong translational initiation site for the 40S ribosomal subunit in plants and other eukaryotes (*31*). (3) The additional N-terminal sequences display characteristics of chloroplast targeting transit peptides: They are devoid of Gly and Pro and deficient in acidic residues, and their middle regions are positively charged and rich in Ser and Thr (*32*−*34*).

We predicted maturation sites at Pro75/Gln76 for ArCCS and Pro90/Glu91 for tCCS, based primarily on the fact that, among precursors of nuclear-encoded chloroplast proteins, the mature protein portions are usually highly homologous between species, while the transit peptides are not. However, it should be noted that these sites may not correspond precisely to the sites used in vivo (*32*).

DNA fragments corresponding to the full-length hCCS, the predicted mature tCCS, and a truncated version of tCCS encoding only domains 2 and 3 (tCCS-D2D3) were amplified by PCR on the templates of pSMCCS plasmid and cDNA clone encoding precursor tomato CCS. The sense primer for hCCS introduced an *Nde*I restriction site at the original AUG translational initiation codon. The sense primers for tCCS and tCCS-D2D3 introduced an *Nde*I restriction site and an AUG codon at Pro90 and Ile166 respectively (numbers refer to the partial sequence of the precursor tCCS; GenBank accession number AF117707). The antisense primers for all three DNA fragments introduced *Bam*HI restriction sites downstream of the termination codons. The resulting DNA fragments encode 274 amino acid full-length hCCS, 221 amino acid predicted mature tCCS, and 145 amino acid polypeptide corresponding to domain 2 and 3 of tCCS starting from Ser167. The PCR products were purified by agarose gel electrophoresis, digested with *Nde*I and *Bam*HI; and ligated into the corresponding sites of pET3a bacterial expression vector (Novagen), which directs expression of the target proteins under the control of the T7 promoter. The integrity and correctness of all cloned DNA was confirmed by nucleotide sequencing.

Protein Expression and Purification. The proteins were expressed in *Escherichia coli* strain BL21(DE3), which houses a genomic copy of T7 RNA polymerase gene under the control of the IPTG inducible *lacUV5* promoter. Cultures (10 L) of cells were grown to an optical density of 0.5−0.8 at 600 nm, the protein expression was initiated by 0.5−0.8 mM IPTG, and cells were harvested after 5−6 h of expression by centrifugation at 4000 rpm for 10 min. The cell pellet was suspended in 100 mL of 50 mM Tris-HCl buffer (pH 8.0) containing 5 mM EDTA, 10 mM DTT; and 50 μg/μL benzamidine (protease inhibitor) and lysed by ultrasonication for 10 cycles of 1 min on/2 min off on ice. SDS−PAGE analyses revealed that hCCS and mature tCCS were mainly present in the soluble fractions, while tCCS-D2D3 was found only in insoluble aggregates known as "inclusion bodies". The cell lysate was centrifuged at 12 000 rpm for 30 min; either the clarified lysate or the inclusion

body pellet was subject to further purification. Solubilization and refolding of tCCS-D2D3 from inclusion bodies was performed as previously described for a blue copper protein, stellacyanin (*26*). Purification of hCCS, tCCS, and tCCS-D2D3 was achieved by anion-exchange chromatography on DEAE-cellulose (Whatman) followed by gel-filtration chromatography on superfine Sephadex G75 or G100 (Pharmacia). Typical anion-exchange chromatography parameters were as follows: 80 mL of DEAE medium was equilibrated with 5 mM Tris-HCl buffer (pH 8.0, containing 5 mM EDTA and 10 mM DTT); protein was eluted with 20 mL of 5 mM Tris-HCl buffer each step, increasing NaCl concentration from 0 to 500 mM in 25 mM increments. Typical gel-filtration chromatography conditions were 450 mL of Sephadex matrix equilibrated with 50 mM Tris-HCl buffer, pH 8.0, containing 50 mM NaCl, 1 mM EDTA, and 5 mM DTT; chromatography was run by gravity with a flow rate of 0.5−1 mL/min. Alternatively, 50 mM sodium phosphate buffer (pH 8.0) was used in place of Tris-HCl buffer in the protein purification preparations. The purity of the proteins was verified by SDS−PAGE and electrospray ionization mass spectrometry. The purified protein from different fractions were pooled and concentrated to a final concentration of approximately 0.5 mM with an Amicon ultrafiltration cell. The purified proteins were stored in −20 °C in 50 mM Tris-HCl or sodium phosphate buffers, pH 8.0, containing 50 mM NaCl, 1 mM EDTA and 5 mM DTT.

The identities of recombinant proteins were confirmed by the electrospray ionization mass spectrometry at UCLA Pasarow Mass Spectrometry Laboratory on a Perkin-Elmer/Sciex API III mass spectrometer equipped with an Ionspray ion source. The experimental mass values 28 911.4 ± 2.3, 23 579.7 ± 2.3, and 15 212.9 ± 1.1 were consistent with the average masses calculated from the amino acid sequence, 29 040.7, 23 578.0, and 15 343.4 for hCCS, tCCS, and tCCS-D2D3, respectively. These masses indicate that the N-terminal Met residue (average mass 131.2) has been cleaved by *E. coli* methionine aminopeptidase in hCCS and tCCS-D2D3, while it remains intact in tCCS.

Metal Titration and Spectroscopy. Proteins for metal titration were transferred into 20 mM phosphate buffer (pH 8.0) by three cycles of 10-fold dilution and subsequent concentration with a Centricon 10 centrifugal filter (Millipore). Protein concentrations were determined by use of the following molar extinction coefficients, which were estimated from the Trp and Tyr content according to ref *35*: ϵ_{280nm} (M^{-1} cm^{-1}) = 12 490 for hCCS and 16 960 for both tCCS and tCCS-D2D3. Typically, a 150 mL aliquot of an approximately 0.3 mM protein solution was titrated with increments of 0.5 equiv of Co^{2+} by adding aliquots of 20 mM cobaltous sulfate solution [$Co(II)SO_4 \cdot 7H_2O$, Mallinckrodt]; the total volume of metal solution added did not exceed 10 mL. Titration end points were reached when the electronic absorption spectra in the visible region remained unchanged upon successive metal additions. Prior to the cobalt titrations, the solutions were incubated under an argon atmosphere in a glovebox (O_2 < 100 ppm) for at least 3 h. Metalation experiments were carried out under an argon atmosphere unless otherwise indicated; the samples were sealed in a microcuvette and transported out of the glovebox before taking a spectrum.

The mercury inhibition experiments, in which appropriate volumes of 20 mM mercuric chloride ($HgCl_2$, Sigma) solution were added prior to the addition of Co^{2+}, were carried out rapidly in air. All of the spectra were taken immediately after the metal ions were added to protein.

Electronic absorption spectra were recorded on a Cary 3 spectrophotometer (Varian, Sunnyvale, CA). Circular dichroism (CD) spectra were recorded at room temperature in air on a Jasco 715 spectropolarimeter (Tokyo, Japan).

The metal ion concentrations were determined by inductively coupled plasma mass spectrometry on a Perkin-Elmer/Sciex Elan 5000A spectrometer at the Environmental Analysis Center, California Institute of Technology. Prior to metal titration experiments, protein samples were analyzed for the presence of metal ions and proved to be virtually metal-free.

RESULTS

Tomato and Arabidopsis CCS. An *Arabidopsis* and several tomato ESTs that displayed remarkable sequence homology to yeast LYS7 and hCCS were identified in GenBank. The nucleotide sequences of the cDNA clones corresponding to *Arabidopsis* and one of the tomato ESTs revealed that they contain 1100 bp and 1162 bp inserts, respectively, and both encode polypeptides of 310 amino acids. These two predicted proteins display more than 80% sequence identity to each other and almost 30% to known CCS sequences (Figure 1). Similar to other CCSs, the predicted mature proteins also consist of three sequence domains, which include an ATX1-like domain, a CuZnSOD-like domain, and a 23−29 amino acid C-terminal domain. In addition, we have shown that both predicted proteins are capable of complementing the aerobic lysine and methionine auxotrophies of a *S. cerevisiae lys7* null strain, evidence that these plant proteins can be considered as functional homologues of CCS (A. Liba, J. Wei, A. M. Nersissian, and J. S. Valentine, unpublished results).

Expression and Purification of CCS Proteins. We successfully expressed the full-length human CCS (hCCS), the full-length tomato CCS (tCCS), and a truncated tomato CCS containing only domain 2 and 3 (tCCS-D2D3) in *E. coli* and purified them to homogeneity, as described in the Experimental Procedures. The yields of purified hCCS, tCCS, and tCCS-D2D3 were approximately 50, 170, and 40 mg/L of bacterial culture, respectively.

Cobalt(2+) Binding to tCCS and hCCS. The electronic absorption spectra for the Co^{2+} titration of tCCS are shown in Figure 2A. When 1 equiv of Co^{2+} was added to tCCS under anaerobic conditions, the resulting spectrum, which appeared immediately upon mixing, had long-wavelength absorption bands, with maxima at 724 and 685 nm and a shoulder at 627 nm, and a shorter-wavelength shoulder peak at 350 nm with much higher intensity (Figure 2Ab). The spectrum remained relatively unchanged after the sample was incubated under argon for 20 h. Full development of this spectrum required 1 equiv of Co^{2+} and the spectrum remained unchanged when additional Co^{2+} was added, i.e., the end point of the Co^{2+} titration was 1 equiv of Co^{2+}/equiv of tCCS. However, when the sample was exposed to air, the long-wavelength bands began decreasing slowly while a new band at 470 nm appeared and kept increasing along with the 350-nm band, and there was a clear isosbestic

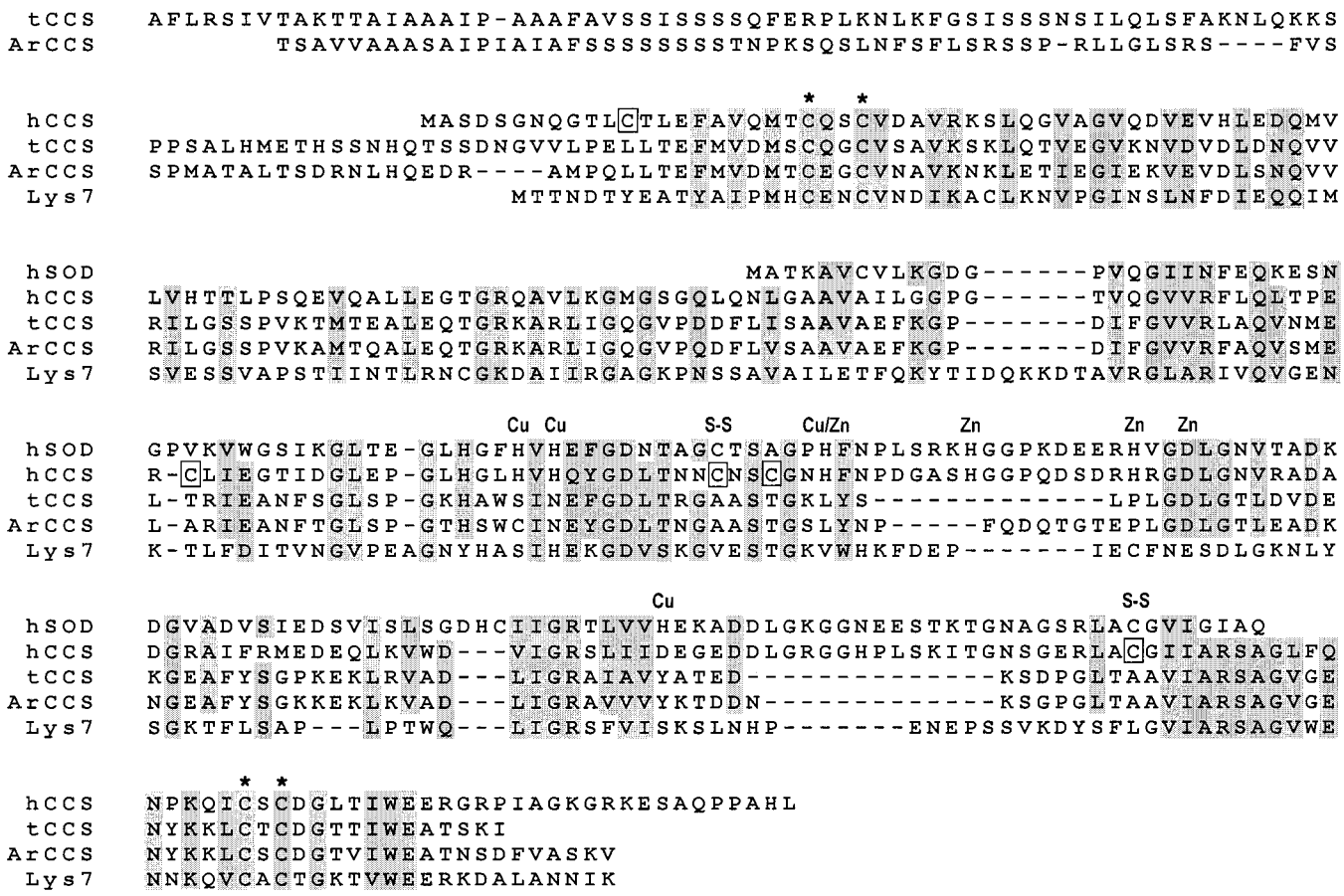

FIGURE 1: Multiple sequence alignment of human, tomato, *Arabidopsis*, and yeast CCS proteins along with human CuZnSOD. The residues that are identical or display conserved side-chain characteristics in at least four sequences are shaded. Four conserved cysteines in all known CCS proteins are indicated by asterisks. Boxes denote the nonconserved cysteines in hCCS. Cu, Zn, and Cu/Zn denote the copper and zinc binding residues in CuZnSOD. S−S denotes cysteines involved in a disulfide bond in CuZnSOD. Dashes indicate gaps that were introduced to optimize the alignment.

point at 650 nm. Spectrum 2Ac is that of the Co^{2+}-tCCS sample exposed to air for 30 min. After 20 h of exposure to air and at 4 °C, the final spectrum was reached (Figure 2Ad).

The UV−vis spectra of Co^{2+} derivatives of tCCS-D2D3 are shown in Figure 2B. Addition of Co^{2+} to tCCS-D2D3 under an argon atmosphere produced a nearly featureless spectrum in the visible region (Figure 2Bb) similar to that of the apoprotein (Figure 2Ba). However, when the sample was exposed to air, the spectrum developed a new peak at 470 nm, the identical position as that seen when Co^{2+}-tCCS was exposed to air, but the long-wavelength bands seen for the full-length protein (Figure 2Ab) were not present (Figure 2Bc).

The UV−vis spectra of Co^{2+} titration of hCCS are shown in Figure 2C. When 1 equiv of Co^{2+} was added to hCCS, the resulting spectrum had a broad band with maximal absorbance at 585 nm with two shoulders at 565 and 530 nm (subsequently referred to as the 585-nm peak), which is very similar to that seen when Co^{2+} is bound to the zinc site of human CuZnSOD (Figure 2Cb) (*36*). When the second equivalent of Co^{2+} was added to hCCS, the resulting spectrum had both the 585-nm peak and the long-wavelength bands (Figure 2Cc) that were also seen in the Co^{2+} titration of tCCS (compare to Figure 2Ab). The spectrum was virtually unchanged after the sample was incubated under argon for 20 h. The spectrum also remained unchanged when Co^{2+} in excess of 2 equiv was added, which indicates that the end point of the Co^{2+} titration was 2 equiv of Co^{2+}/equiv of hCCS. The Co^{2+} derivatives of hCCS were more oxygen-sensitive compared to that of tCCS. When the sample was exposed to air, the long-wavelength bands decreased and a new peak at 470 nm appeared. After incubation in air and on ice for approximately 40 min, the long-wavelength bands almost completely disappeared, and the 470-nm peak reached its maximum absorbance (Figure 2Cd).

The CD spectra in the visible region for Co^{2+} titration of tCCS are shown in Figure 3A. The spectrum of the apo-tCCS protein was a flat line (Figure 3Aa). Addition of 1 equiv of Co^{2+} resulted in a spectrum with three peaks, a positive band at 620 nm, a negative band at 520 nm, and a positive band at 395 nm (Figure 3Ab). Addition of Co^{2+} in excess of 1 equiv did not change the spectrum further, again supporting an end point of 1 equiv of Co^{2+}/equiv of tCCS. Though the UV−visible spectrum of tCCS appeared to be oxygen-sensitive and changed over time when exposed to air, the CD spectrum of tCCS was nearly unchanged even when the Co^{2+}-tCCS sample was exposed to air for 20 h. The resulting CD spectrum when Co^{2+} was added to tCCS-D2D3 had the same three peaks as that of the full-length tCCS, though the intensities of all three peaks were lower (Figure 3Ac).

The CD spectra in the visible region for Co^{2+} titration of hCCS are shown in Figure 3B. The first equivalent of Co^{2+} added to hCCS produced a flat line (Figure 3Bb) similar to

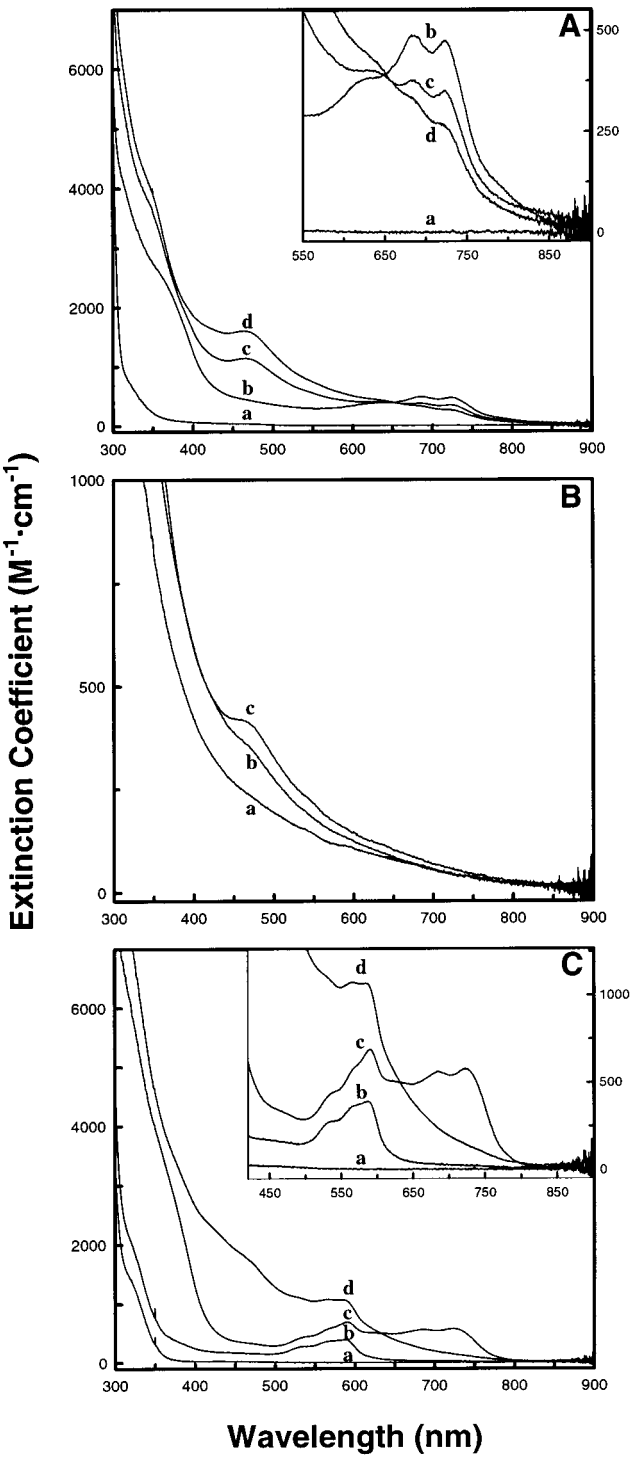

FIGURE 2: Electronic absorption spectra of Co^{2+} derivatives of human and tomato CCS. (A) Electronic absorption spectra of tCCS: (a) metal-free tCCS; (b) tCCS with 1 equiv of Co^{2+} added anaerobically; (c) sample b exposed to air for 30 min; (d) sample b exposed to air for 20 h. (B) Electronic absorption spectra of tCCS-D2D3: (a) metal-free tCCS-D2D3; (b) tCCS-D2D3 with 1 equiv of Co^{2+} added anaerobically; (c) sample b exposed to air. (C) Electronic absorption spectra of hCCS: (a) metal-free hCCS; (b) hCCS with 1 equiv of Co^{2+} added anaerobically; (c) hCCS with 2 equiv of Co^{2+} added anaerobically; (d) sample c exposed to air for 40 min.

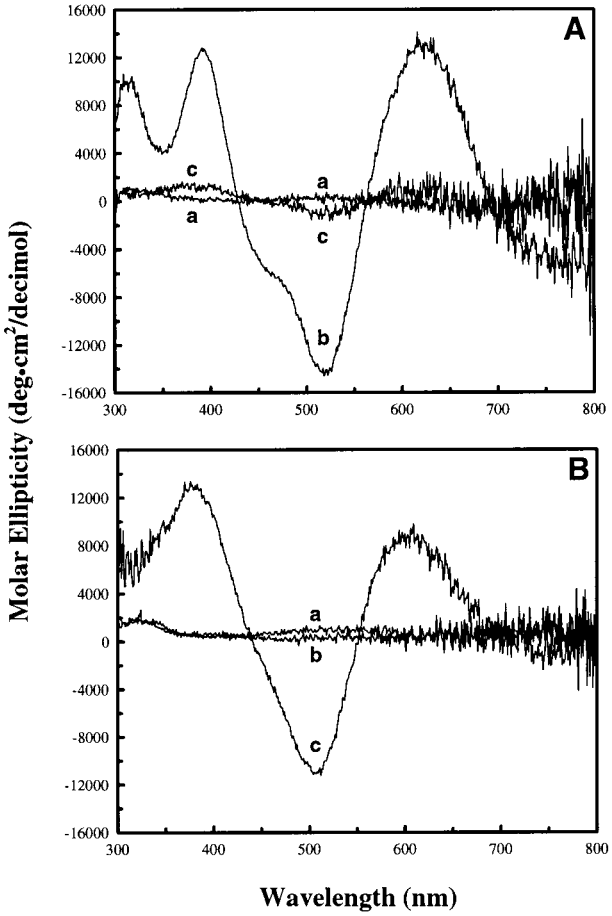

FIGURE 3: Circular dichroism spectra of Co^{2+} derivatives of human and tomato CCS. (A) Circular dichroism spectra of tCCS: (a) metal-free tCCS; (b) tCCS with 1 equiv of Co^{2+} added; (c) tCCS-D2D3 with 1 equiv of Co^{2+} added. (B) Circular dichroism spectra of hCCS: (a) metal-free hCCS; (b) hCCS with 1 equiv of Co^{2+} added; (c) hCCS with 2 equiv of Co^{2+} added to hCCS.

that of the apoprotein (Figure 3Ba), despite the fact that the 585-nm peak appeared in the UV−vis spectrum. The second equivalent of Co^{2+} produced a CD spectrum with three peaks, a positive band at 610 nm, a negative band at 505 nm, and a positive band again at 380 nm (Figure 3Bc), which was nearly identical to that seen in the case of Co^{2+}-tCCS. Thus the visible region CD signals are due to the second Co^{2+} ion bound to hCCS. Addition of Co^{2+} in excess of 2 equiv did not change the spectrum further, again supporting an end point of 2 equiv of Co^{2+}/equiv of hCCS.

Inhibition of Cobalt(2+) Binding by Mercury(2+). The Co^{2+} spectrum of tCCS under anaerobic conditions is highly reminiscent of the spectra of Co^{2+} coordination complexes or Co^{2+}-substituted metalloproteins in which Co^{2+} is bound in a tetrahedral geometry to multiple thiolate ligands (see Discussion) (*29, 37*−*41*). Examination of the tCCS sequence revealed a total of four cysteine residues, all conserved in the CCS family, two in the consensus metal binding MXCXXC motif in the ATX1-like domain 1 and two in domain 3. To test for the involvement of thiolate ligands in binding Co^{2+}, mercuric ion, Hg^{2+}, which has a high affinity for thiolates, was added to tCCS prior to the addition of Co^{2+} in an attempt to block the cysteine residues that are possible ligands for Co^{2+} binding.

Addition of 1 equiv of Co^{2+} to apo-tCCS under either anaerobic or aerobic conditions resulted in the immediate appearance of the long-wavelength bands. Under aerobic conditions, the long-wavelength bands then decreased in intensity while the 470-nm peak appeared (Figure 4Aa). Addition of 1 equiv of Hg^{2+} prior to Co^{2+} addition to tCCS

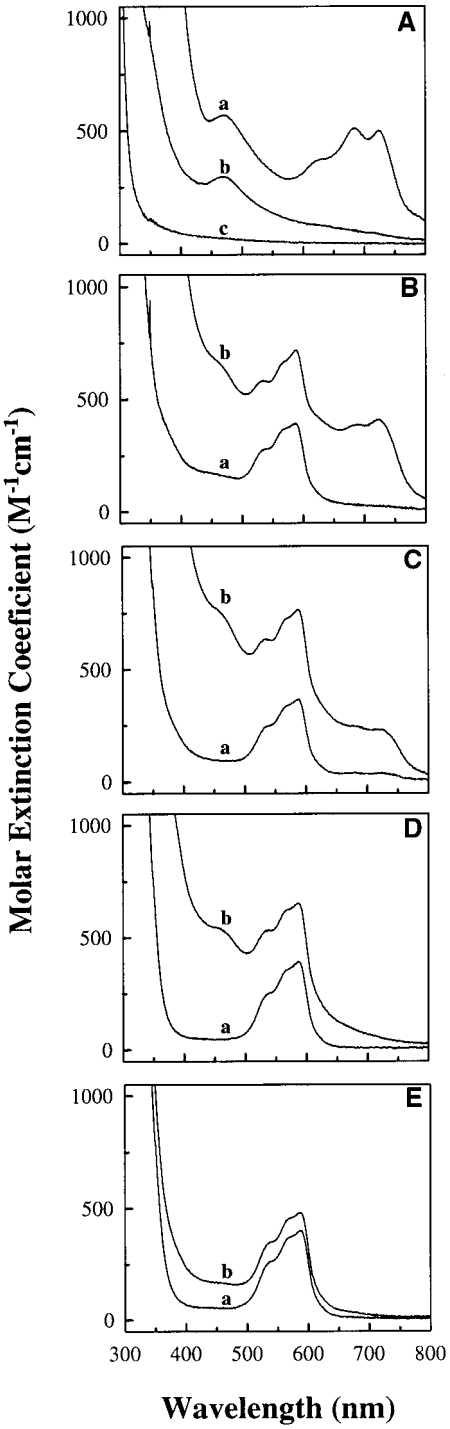

FIGURE 4: Electronic absorption spectra of Hg^{2+} inhibition of Co^{2+} binding to human and tomato CCS under aerobic conditions. Spectra were taken immediately after the metal ion solutions were added to the protein solution. (A) Hg^{2+} inhibition of Co^{2+} binding to tCCS: (a) 1 equiv of Co^{2+} was added to tCCS with no prior addition of Hg^{2+}; (b) 1 equiv of Co^{2+} was added to tCCS with prior addition of 1 equiv of Hg^{2+}; (c) 1 equiv of Co^{2+} was added to tCCS with prior addition of 2 equiv of Hg^{2+}. (B) Spectra of Co^{2+} derivatives of hCCS with no prior addition of Hg^{2+}: (a) 1 equiv of Co^{2+} was added to hCCS; (b) 2 equiv of Co^{2+} was added to hCCS. (C) Spectra of Co^{2+} derivatives of hCCS with prior addition of 1 equiv of Hg^{2+}: (a) 1 equiv of Co^{2+} was added to hCCS; (b) 2 equiv of Co^{2+} was added to hCCS. (D) Spectra of Co^{2+} derivatives of hCCS with prior addition of 2 equiv of Hg^{2+}: (a) 1 equiv of Co^{2+} was added to hCCS; (b) 2 equiv Co^{2+} was added to hCCS. (E) Spectra of Co^{2+} derivatives of hCCS with prior addition of 3 equiv of Hg^{2+}: (a) 1 equiv of Co^{2+} was added to hCCS; (b) 2 equiv of Co^{2+} was added to hCCS.

under aerobic conditions completely suppressed the formation of the long-wavelength bands but not of the 470-nm band, although the 470-nm band had a significantly lower absorbance (Figure 4Ab). This spectrum was nearly identical to that seen when the Co^{2+} derivative of tCCS-D2D3 was exposed to air (compare to Figure 2Bc). Addition of 2 equiv of Hg^{2+} to tCCS, prior to Co^{2+} addition, completely eliminated the appearance of both the long-wavelength bands and the 470-nm peak (Figure 4Ac). Prior addition of 1 equiv of Hg^{2+} to tCCS-D2D3 also blocked development of the 470-nm band and produced a featureless spectrum similar to Figure 4Ac.

Mercury inhibition experiments were also carried out with hCCS under aerobic conditions; the spectra are shown in Figure 4B−E. There are five additional cysteine residues in hCCS besides the four conserved ones, one in the ATX1-like domain 1 and four in the CuZnSOD-like domain 2. Not surprisingly, more equivalents of Hg^{2+} were therefore required to block Co^{2+} binding than in the case of tCCS.

Addition of 2 equiv of Co^{2+} to apo-hCCS under either anaerobic or aerobic conditions results in the immediate appearance of both the 585-nm and the long-wavelength bands. Under aerobic conditions, the long-wavelength bands then decreased in intensity and the 470-nm peak appeared (Figure 4Bb). Prior addition of 1 equiv of Hg^{2+} to hCCS had little effect on the Co^{2+} titration (compare Figure 4 panels B and C), suggesting that the first equivalent of Hg^{2+} was bound to one or more cysteine residues not involved in Co^{2+} binding. By contrast, prior addition of 2 equiv of Hg^{2+} did influence the results of the Co^{2+} titration of hCCS. The spectrum of hCCS after addition of 2 equiv of Hg^{2+} and one of Co^{2+} was almost identical to that in the absence of Hg^{2+} (Figure 4Da). When the second equivalent of Co^{2+} was added, however, the 470-nm peak appeared without any evidence for the long-wavelength bands (Figure 4Db). The absence of the long-wavelength bands in the cobalt titration after addition of 2 equiv of Hg^{2+} is similar to the absence of the same band after 1 equiv of Hg^{2+} had been added to tCCS (compare spectra b in Figure 4 panels D and A). Three equivalents of Hg^{2+} once again had little or no effect on the subsequent binding of the first equivalent of Co^{2+} (Figure 4Ea) but completely inhibited the appearance of both the long-wavelength bands and the 470-nm peak upon the addition of the second equivalent of Co^{2+} (Figure 4Eb).

When more than 3 equiv of Hg^{2+} was added to hCCS, the long-wavelength bands and the 470-nm peak were both completely inhibited. Moreover, the 585-nm peak also diminished in intensity. Addition of 5 equiv of Hg^{2+} eliminated all Co^{2+} peaks, and the spectrum was just a flat line in the visible region (data not shown).

DISCUSSION

We selected tomato CCS for comparative studies with hCCS for the following reasons. The mature tCCS is composed of 220 amino acid residues and appears to be the smallest CCS identified to date, compared to 274 for its human and 249 for yeast counterparts. Like Lys7, it does not possess any SOD-like metal binding site in domain 2, and its only cysteine residues are the four conserved ones, two in the consensus metal binding MXCXXC motif in domain 1 and two in domain 3. We anticipated that these

sequence characteristics would promote its in vitro stability and eliminate extraneous metal binding, making it an excellent candidate for biophysical and biochemical studies.

Titration of tCCS with Co^{2+} gave a clear end point of 1 Co^{2+}/tCCS protein. The spectrum of Co^{2+}-tCCS under anaerobic conditions (Figure 2Ab), with long-wavelength bands at 724, 685, and 627 nm and a strong shoulder band at 350 nm, is remarkably similar to those seen in Co^{2+}-rubredoxin (*39*) and Co^{2+} in the noncatalytic site of liver alcohol dehydrogenase (*40*), both of which bind Co^{2+} in a tetrahedral geometry consisting of four cysteine thiolate ligands. They also strongly resemble the spectra of some well-characterized tetrathiolate coordination complexes of Co^{2+} (*39, 41*). The positions and intensities of the long-wavelength bands are characteristic of a high-spin Co^{2+} in a distorted tetrahedral environment and are assigned to the spin-allowed ligand field transitions $^4A_2 \rightarrow {}^4T_1(P)$ (*38, 39*). The intense band at 350 nm is assigned to a S → Co charge-transfer band; similar bands are seen also in Co^{2+}-rubredoxin, Co^{2+}-liver alcohol dehydrogenase, Co^{2+}-stellacyanin, and the Co^{2+}-tetrathiolate complex $[Co(S_2\text{-}o\text{-}xyl)_2]^{2-}$ (*39*−*41*). The spectrum of Co^{2+}-tCCS thus strongly resembles those of a number of well-characterized Co^{2+}-tetrathiolate complexes, $Co^{2+}S_4$; it is less similar to tetrahedral complexes with three sulfur ligands, e.g., $Co^{2+}S_3N$; and it differs substantially from those with two or one sulfur ligand, e.g., $Co^{2+}S_2N_2$ or Co^{2+}-SN_3 (*29, 37*−*39, 41*).

Within the entire sequence of tCCS, there are only four cysteine residues, two each in domains 1 and 3. If we accept the conclusion, based on the UV−vis spectra, that Co^{2+}-tCCS contains a high-spin, distorted tetrahedral Co^{2+} bound to a S_4 or possibly a S_3X ligand set, we must conclude that cysteines from both domains 1 and 3 are binding to one Co^{2+} ion. Further evidence came from the anaerobic Co^{2+} titration of the truncated protein lacking domain1, tCCS-D2D3, whose spectrum is completely featureless (Figure 2Bb). It suggests that the spectrum characteristic of Co^{2+}-tetrathiolate coordination cannot be achieved when only two cysteines in domain 3 are present, i.e., it requires domain 1, more specifically, the two cysteine residues in domain 1.

While domain 2 of tCCS does not possess any obvious potential metal binding sites, domain 2 of hCCS has an intact (SOD-like) zinc binding site, and the copper binding site is only slightly altered. The 585-nm peak that was observed when 1 equiv of Co^{2+} was added to hCCS is very similar to that of Co^{2+} bound at the zinc site of CuZnSOD, with respect to its position, shape, and intensity (see Figure 2Cb) (*36*). This peak was never observed in the Co^{2+} titration of tCCS. Therefore, the 585-nm peak of Co^{2+}-hCCS is assigned to Co^{2+} binding in domain 2, most likely at the site analogous to the zinc site of CuZnSOD. The difference spectrum of $(Co^{2+})_2$-hCCS minus Co^{2+}-hCCS (Figure 5b) closely resembles the spectrum of Co^{2+}-tCCS under anaerobic conditions (Figure 5a, the same as Figure 2Ab), which strongly suggests that Co^{2+} binds to hCCS in the same fashion, by coordinating with three or four cysteines in a distorted tetrahedral geometry (Scheme 1).

The visible CD spectra of the titration of tCCS and hCCS with Co^{2+} had clear end points at 1 and 2 equiv, respectively. The first Co^{2+} ion bound to hCCS was silent in its visible CD spectrum, although it had a well-defined 585-nm peak in its electronic absorption spectrum. The one Co^{2+} bound

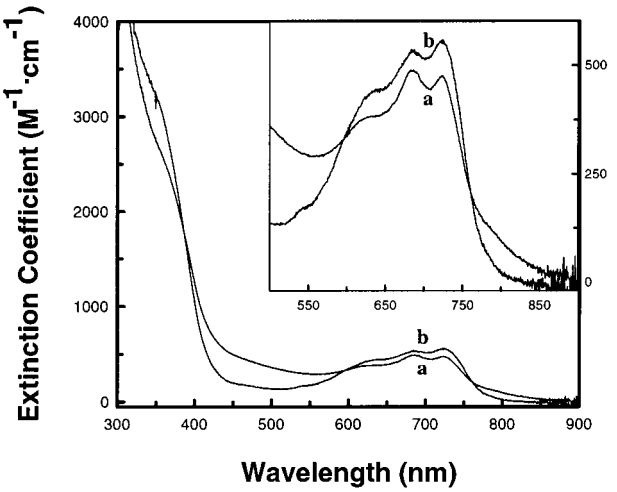

FIGURE 5: Electronic absorption spectrum of Co^{2+}-tCCS (a) and the difference spectrum of $(Co^{2+})_2$-hCCS minus Co^{2+}-hCCS (b).

Scheme 1: Schematic Diagram of Co^{2+} Binding Sites in Human CCS[a]

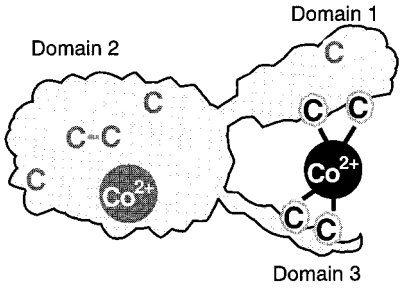

[a] The four cysteine residues conserved in the CCS family are shown in black, while the extra five nonconserved cysteine residues found in human CCS are shown in gray. The Co^{2+} bound in the metal binding site shared by both human and tomato CCS is shown in black, coordinating to four conserved cysteine residues from both domains 1 and 3. The Co^{2+} that binds only to hCCS in the site resembling the zinc site of CuZnSOD is shown in gray.

to tCCS and the second Co^{2+} bound to hCCS produced very similar visible CD spectra. We presume that this Co^{2+} binds to cysteines from both domains 1 and 3 in tCCS and hCCS.

The Co^{2+} derivatives of both CCS proteins were found to be air-sensitive. When exposed to air, a new peak at 470 nm consistently appeared. The assignment of the 470-nm peak, which has also been observed in Co^{2+}-rubredoxin (*39*), is less certain. In the literature (*39*), it has been assigned as a charge-transfer transition of a cobaltous-thiolate complex. However, in this study, the 470-nm peak was completely absent under anaerobic conditions. We speculate that oxidation of the liganding thiolate groups by dioxygen is mediated by the presence of Co^{2+} and that the 470-nm peak results from charge transfer between the oxidized thiolate ligands and cobalt.

The observation that the CD spectra did not change after the Co^{2+} derivatives were exposed to air indicates that Co^{2+} was still bound to the protein after the reaction that produced the 470-nm band and that the geometry of the Co^{2+} ion binding was not significantly altered, despite the fact that the thiolate ligands in the cysteine residues may have been oxidized.

The electronic absorption spectra of Co^{2+} derivatives of tCCS and hCCS under anaerobic conditions suggest strongly

that Co^{2+} is binding to three or four cysteine ligands in a distorted tetrahedral geometry. Two conserved cysteines in domain 1 are in a putative heavy metal binding motif, MXCXXC, which has been demonstrated to coordinate with metal ions in several different proteins (*16*, *17*, *19*). The absence of the long-wavelength bands and the virtually featureless spectrum of Co^{2+}-tCCS-D2D3 observed under anaerobic conditions strongly suggests that the cysteines in domain 1 are involved in binding Co^{2+} in full-length tCCS. If Co^{2+} does indeed have an S_3X or S_4 ligand environment in the Co^{2+}-CCS complexes, the other possible thiolate ligands must be one or both of two other conserved cysteines in domain 3. The two cysteines in domain 3 are separated by only one residue; such a CXC motif has been found to bind to a metal ion in 35 cases out of 553 protein entries of the Brookhaven Protein Data Bank containing CXC sequences (*42*, *43*). In addition, the 470-nm peak that appeared when Co^{2+}-tCCS-D2D3 was exposed to air was also observed in Co^{2+} titration of tCCS and hCCS under aerobic conditions. The partial retention of the 470-nm peak in the spectrum of Co^{2+}-tCCS-D2D3 suggests that the CXC motif in domain 3 is involved in Co^{2+} binding and the development of the peak. We conclude that either three or four cysteines are coordinating to Co^{2+}, i.e., domains 1 and domain 3 are directly interacting by coordinating to the same metal ion (Scheme 1).

Addition of different amounts of mercuric ion, Hg^{2+}, to tCCS or hCCS prior to the Co^{2+} titration provided additional supporting evidence concerning the identity of the cysteines involved in binding to Co^{2+}. In the case of tCCS, which binds only 1 equiv of Co^{2+}, 2 equiv of Hg^{2+} was nevertheless required to inhibit Co^{2+} binding completely. Binding of Co^{2+} to Hg^{2+}-tCCS produced a spectrum that was nearly identical to that seen in Co^{2+}-tCCS-D2D3 exposed to air, with a band at 470 nm but not the long-wavelength bands (compare Figure 4Ab to Figure 2Bc). Thus prior addition of 1 equiv of Hg^{2+} did not completely block Co^{2+} binding but clearly changed the nature of the Co^{2+} binding site to one that closely resembles that of Co^{2+}-tCCS-D2D3 in air. We conclude that the first equivalent of Hg^{2+} binds to two cysteine residues in the ATX1-like domain 1, in a fashion similar to that observed for the Hg^{2+} complex of yeast ATX1 itself (*19*). The absence of any long-wavelength bands when Co^{2+} was added to Hg^{2+}-tCCS or once again supports our hypothesis that cysteines in domain 1 are involved in the binding of Co^{2+} to full-length tCCS.

In the case of hCCS, binding of Co^{2+} to Hg^{2+}-hCCS produced spectra that were little changed from those observed in the absence of Hg^{2+} (compare Figure 4 panels C and B); thus we conclude that the first Hg^{2+} binds predominantly to cysteine residues(s) not involved in Co^{2+} binding. Examination of hCCS sequence reveals five additional cysteine residues that are not conserved in the CCS family (see Figure 1). Cys12 (numbers refer to the full-length hCCS sequence) in domain 1 is expected to be exposed on the protein surface since it is in the analogous position to Tyr7 in Lys7 which is solvent exposed (*21*) and thus is the most likely target of the first equivalent of Hg^{2+}. By their positions in the sequence alignment, Cys141 and Cys227 in the CuZnSOD-like domain 2 are likely to form a disulfide bond, and the side chains of Cys113 and Cys144 are likely to be buried inside the protein.

Binding of 1 equiv of Co^{2+} to $(Hg^{2+})_2$-hCCS resulted in the appearance of the band at 585 nm which we have assigned to domain 2 (Figure 4Da). Addition of the second Co^{2+} resulted in absorbance at 470 nm but the long-wavelength bands did not appear (compare spectra b in Figure 4 panel D with those in panels B and C); thus the behavior observed is similar to that previously described for Co^{2+} binding to Hg^{2+}-tCCS and tCCS-D2D3 (Figures 4Ab and 2Bc), and we conclude that the second Hg^{2+} is also binding to Cys22 and Cys25 in the ATX1-like domain 1 in the case of hCCS.

When Co^{2+} was added to $(Hg^{2+})_3$-hCCS, the first equivalent once again gave the 585-nm band tentatively assigned to domain 2 (Figure 4Ea). The binding of the second equivalent of Co^{2+} produced relatively little change in the spectrum, which has neither the 470-nm peak nor the long-wavelength bands (Figure 4Eb). This suggests to us that the third Hg^{2+} is binding to domain 3 of hCCS in the same fashion as the second Hg^{2+} was bound to tCCS. Addition of 5 equiv of Hg^{2+} completely eliminated evidence for subsequent binding of Co^{2+} to hCCS at any Co^{2+} concentrations we employed (up to 6 equiv).

Several of our observations are potentially relevant to the mechanism of action of tCCS and hCCS in enabling the proper metalation of CuZnSOD in vivo. First, the involvement of both domains 1 and 3 in binding Co^{2+} suggests that these domains may function in concert in binding copper and/or zinc ions during the metal delivery process. Second, the fact that yeast Lys7 and tomato CCS do not possess any metal binding sites in domain 2 and that the metal ion binding behavior of hCCS, apart from the binding to its domain 2, is very similar to that of tCCS suggests common mechanisms for metal ion delivery involving predominantly domains 1 plus 3.

NOTE ADDED IN PROOF

We have recently found the genomic sequence for *Arabidopsis* CCS in a BAC clone from chromosome 1 (GenBank accession number AC025417). The translational initiation site is located 10 amino acids upstream of the sequence reported in this study (see Figure 1) and the missing part of the sequence is MASILRSVAT.

ACKNOWLEDGMENT

We thank Dr. Valeria C. Culotta for generously providing pSMCCS plasmid, Dr. Kym Faull for assistance in mass spectrometry, and Dr. Martin Philips for help with circular dichroism measurement. We also thank a reviewer for a valuable suggestion.

REFERENCES

1. Culotta, V. C., Klomp, L. W. J., Strain, J., Casareno, R. L. B., Krems, B., and Gitlin, J. D. (1997) *J. Biol. Chem. 272*, 23469−72.
2. Valentine, J. S., and Gralla, E. B. (1997) *Science 278*, 817−8.
3. Harrison, M. D., Jones, C. E., Solioz, M., and Dameron, C. T. (2000) *Trends Biochem. Sci. 25*, 29−32.
4. Bhattacharjee, J. K., Tucci, A. F., and Strassman, M. (1968) *Arch. Biochem. Biophys. 123*, 235−9.
5. Horecka, J., Kinsey, P. T., and Sprague, G. F., Jr. (1995) *Gene 162*, 87−92.

6. Gamonet, F., and Lauquin, G. J. (1998) *Eur. J. Biochem. 251*, 716−23.
7. Lyons, T. J., Nersissian, A., Goto, J. J., Zhu, H., Gralla, E. B., and Valentine, J. S. (1998) *J. Biol. Inorg. Chem. 3*, 650−662.
8. Lin, S.-J., and Culotta, V. C. (1995) *Proc. Natl. Acad. Sci. U.S.A. 92*, 3784−8.
9. Pufahl, R. A., Singer, C. P., Peariso, K. L., Lin, S.-J., Schmidt, P. J., Fahrni, C. J., Culotta, V. C., Penner-Hahn, J. E., and O'Halloran, T. V. (1997) *Science 278*, 853−6.
10. Klomp, L. W. J., Lin, S.-J., Yuan, D. S., Klausner, R. D., Culotta, V. C., and Gitlin, J. D. (1997) *J. Biol. Chem. 272*, 9221−6.
11. Himelblau, E., Mira, H., Lin, S.-J., Culotta, V. C., Penarrubia, L., and Amasino, R. M. (1998) *Plant Physiol. 117*, 1227−34.
12. Sahlman, L., and Jonsson, B. H. (1992) *Eur. J. Biochem. 205*, 375−81.
13. Silver, S., Nucifora, G., Chu, L., and Misra, T. K. (1989) *Trends. Biochem. Sci. 14*, 76−80.
14. Vulpe, C. D., and Packman, S. (1995) *Annu. Rev. Nutr. 15*, 293−322.
15. Vulpe, C., Levinson, B., Whitney, S., Packman, S., and Gitschier, J. (1993) *Nat. Genet. 3*, 7−13.
16. Steele, R. A., and Opella, S. J. (1997) *Biochemistry 36*, 6885−95.
17. Qian, H., Sahlman, L., Eriksson, P.-O., Hambraeus, C., Edlund, U., and Sethson, I. (1998) *Biochemistry 37*, 9316−22.
18. Gitschier, J., Moffat, B., Reilly, D., Wood, W. I., and Fairbrother, W. J. (1998) *Nat. Struct. Biol. 5*, 47−54.
19. Rosenzweig, A. C., Huffman, D. L., Hou, M. Y., Wernimont, A. K., Pufahl, R. A., and O'Halloran, T. V. (1999) *Struct. Fold. Des. 7*, 605−17.
20. Lamb, A. L., Wernimont, A. K., Pufahl, R. A., O'Halloran, T. V., and Rosenzweig, A. C. (2000) *Biochemistry 39*, 1589−1595.
21. Hall, L. T., Sanchez, R. J., Holloway, S. P., Zhu, H., Stine, J. E., Lyons, T. J., Demeler, B., Schirf, V., Hansen, J. C., Nersissian, A. M., Valentine, J. S., and Hart, P. J. (2000) *Biochemistry 39*, 3611−3623.
22. Lamb, A. L., Wernimont, A. K., Pufahl, R. A., Culotta, V. C., O'Halloran, T. V., and Rosenzweig, A. C. (1999) *Nat. Struct. Biol. 6*, 724−9.
23. Schmidt, P. J., Rae, T. D., Pufahl, R. A., Hamma, T., Strain, J., O'Halloran, T. V., and Culotta, V. C. (1999) *J. Biol. Chem. 274*, 23719−25.
24. Brown, R. H., Jr. (1998) *Nat. Med. 4*, 1362−4.
25. Goto, J. J., Zhu, H., Sanchez, R. J., Nersissian, A., Gralla, E. B., Valentine, J. S., and Cabelli, D. E. (2000) *J. Biol. Chem. 275*, 1007−1014.
26. Nersissian, A. M., Mehrabian, Z. B., Nalbandyan, R. M., Hart, P. J., Fraczkiewicz, G., Czernuszewicz, R. S., Bender, C. J., Peisach, J., Herrmann, R. G., and Valentine, J. S. (1996) *Protein Sci. 5*, 2184−92.
27. Hart, P. J., Nersissian, A. M., Herrmann, R. G., Nalbandyan, R. M., Valentine, J. S., and Eisenberg, D. (1996) *Protein Sci. 5*, 2175−83.
28. Nersissian, A. M., Immoos, C., Hill, M. G., Hart, P. J., Williams, G., Herrmann, R. G., and Valentine, J. S. (1998) *Protein Sci. 7*, 1915−29.
29. Maret, W., and Vallee, B. L. (1993) *Methods Enzymol. 226*, 52−71.
30. Bertini, I., Mangani, S., and Viezzoli, M. S. (1998) *Adv. Inorg. Chem. 45*, 127−250.
31. Kozak, M. (1999) *Gene 234*, 187−208.
32. Emanuelsson, O., Nielsen, H., and von Heijne, G. (1999) *Protein Sci. 8*, 978−84.
33. Soll, J., and Tien, R. (1998) *Plant Mol. Biol. 38*, 191−207.
34. Robinson, C., Hynds, P. J., Robinson, D., and Mant, A. (1998) *Plant Mol. Biol. 38*, 209−21.
35. Pace, C. N., Vajdos, F., Fee, L., Grimsley, G., and Gray, T. (1995) *Protein Sci. 4*, 2411−23.
36. Lyons, T. J., Liu, H., Goto, J. J., Nersissian, A., Roe, J. A., Graden, J. A., Cafe, C., Ellerby, L. M., Bredesen, D. E., Gralla, E. B., and Valentine, J. S. (1996) *Proc. Natl. Acad. Sci. U.S.A. 93*, 12240−4.
37. Faller, P., and Vasak, M. (1997) *Biochemistry 36*, 13341−8.
38. Vasak, M. (1980) *J. Am. Chem. Soc. 102*, 3953−55.
39. May, S. W., and Kuo, J. Y. (1978) *Biochemistry 17*, 3333−8.
40. Maret, W., Andersson, I., Dietrich, H., Schneider-Bernlohr, H., Einarsson, R., and Zeppezauer, M. (1979) *Eur. J. Biochem. 98*, 501−12.
41. Lane, R. W., Ibers, J. A., Frankel, R. B., Papaefthymiou, G. C., and Holm, R. H. (1977) *J. Am. Chem. Soc. 99*, 84−98.
42. Falconi, M., Iovino, M., and Desideri, A. (1999) *Struct. Fold. Des. 7*, 903−8.
43. Bernstein, F. C., Koetzle, T. F., Williams, G. J. B., Meyer, E. F., Jr., Brice, M. D., Rodgers, J. R., Kennard, O., Shimanouchi, T., and Tasumi, M. (1977) *J. Mol. Biol. 112*, 535−42.

BI992727+